



**HAL**  
open science

# Numerical approach using DEM to control the mechanical strength of pharmaceutical tablets

Hamza Haddad, Willy Leclerc, Mohamed Guessasma

► **To cite this version:**

Hamza Haddad, Willy Leclerc, Mohamed Guessasma. Numerical approach using DEM to control the mechanical strength of pharmaceutical tablets. 15ème colloque national en calcul des structures, Université Polytechnique Hauts-de-France [UPHF], May 2022, 83400 Hyères-les-Palmiers, France. hal-03717669

**HAL Id: hal-03717669**

**<https://hal.science/hal-03717669>**

Submitted on 8 Jul 2022

**HAL** is a multi-disciplinary open access archive for the deposit and dissemination of scientific research documents, whether they are published or not. The documents may come from teaching and research institutions in France or abroad, or from public or private research centers.

L'archive ouverte pluridisciplinaire **HAL**, est destinée au dépôt et à la diffusion de documents scientifiques de niveau recherche, publiés ou non, émanant des établissements d'enseignement et de recherche français ou étrangers, des laboratoires publics ou privés.

# Numerical approach using DEM to control the mechanical strength of pharmaceutical tablets

H. Haddad<sup>1</sup>, W. Leclerc<sup>1</sup>, M. Guessasma<sup>1</sup>

<sup>1</sup> LTI, Université de Picardie Jules Verne, hamza.haddad@u-picardie.fr

**Abstract** — The present contribution deals with a discrete Element Method (DEM) based on a hybrid particulate lattice model to predict the mechanical strength of pharmaceutical tablets. We consider the classical approach based on the Stress Concentration Force (SCF) obtained at a defect of controlled size. The paper aims at studying the benefits of such a concepts to provide suitable mechanical strength through diamteral compression tests of a cylindrical tablets with a hole. Results exhibited that ratio of 3 between hole and tablet radii is required to obtained proper mechanical strength.

**Mots clés** — DEM, Pharmaceutical tabletes, mechanical strength, SCF.

## 1 Introduction

Powders are the most common used materials in the planet that many industries such as food, cosmetics and drug deal with handling and processing them. However, some problems related to the physical and mechanical properties of powder or process parameters can arise during the process leading to non-conformity of the tablets. The most important problems in the pharmaceutical industry are: copping of tablets, adherence or sticking of powder to the wall, low mechanical resistance or bad dissolution of tablets. controlling the behavior of powders during the manufacturing process is of crucial challenges for industries and researchers alike. The complexity of the powder interactions stills a barrier to obtain relevant models adapted to the different processes and situations. Empirical solutions are often used. Nevertheless, the precision and reproducibility of powder processes are crucial.

Understanding the link between powder properties and mechanical strength of tablets is a major step forward in establishing criteria for optimizing the compression and processing properties. The classical approach used in pharmaceutical fields is based on the Stress Concentration Force (SCF) obtained at a defect of controlled size. Mechanical strength of such material depends on its capability to relieve stress concentration. The diametral compression of tablets with a cylindrical hole test is often used. This approach was introduced in the pharmaceutical field by Hiestand et al. [1]. Review of pharmaceutical literature shows that there is no consensus on the influence of the ratio between the radius of the hole and the radius of the tablet on its mechanical strength [2, 3]. This gives rise to contradictory results concerning the SCF value [4, 5]. Furthermore, we consider that tablets are subjected to relatively homogeneous stresses which is not true. However, tablets are characterized by structural defaults and porous state.

To overcome the limits of the exsting modeling, we aim to develop a numerical methodology based on the Discrete Element Method (DEM) to optimize the compression process and control the mechanical performances of pharmaceutical tablets. The DEM is a promising tool to model compression process, from powder bed to the characterization of mechanical properties. Such an approach has been applied to simulate mechanical behavior of cohesive granular media [6]. Besides, Moukadiri et al. [7] developed a DEM-based approach called halo to study the level of dispersion of the stress obtained at the scale of the particle which is always heterogeneous, even if it is theoretically homogeneous. Leclerc et al. [8] show the suitability of the DEM to simulate cracks initiation and propagation in cohesive granular media.

Following the present introduction, the paper is outlined as follows. Section 2 describes the hybrid lattice-particle model used to simulate a cohesive granular medium and the halo approach to determine

the level of stress dispersion. In section 3, diametral compression test of pharmaceutical tablet is carried out. Results are in agreement with theoretical solutions in terms of stress fields. In section 4, the influence of ratio between hole and tablet radii on the mechanical strength is investigated. A Special care is taken to accurate control the dispersity of stress fields.

## 2 Hybrid lattice-particle model

### 2.1 Particulate system

We consider the hybrid lattice-particle model [9] for which a continuous medium is represented using a twofold, particulate and lattice, description. Particulate systems are random granular packings composed of spherical particles in point contact. Some intrinsic features of the particulate system such as the volume fraction of particles  $\phi$ , the cardinal number  $Z$ , and the isotropy of the particulate system impact on the modelling of a continuous medium so that a great care is taken to control these parameters during the generation process. In the present contribution, our choice is to target the characteristics of a Random Close Packing (RCP) which is related to a volume fraction  $\phi$  of 0.64 and a cardinal number  $Z$  of 6.2. Nevertheless, based on the findings of previous studies [10], the system is willingly densified to a higher value of 7.5 to avoid undesirable effects due to very low local cardinal numbers (less than 3). The isotropy of the particulate system is ensured by introducing a small polydispersity controlled by the coefficient of variation, i.e. the ratio of the standard deviation to the mean particle radius, which is set to 0.3 in this work.

### 2.2 Cohesive beam model

Cohesive forces are introduced at the scale of the interparticle contact to simulate a continuous medium. In the present contribution, we opt for a cohesive beam model based on Euler-Bernoulli formulation [9] which proved to be more suitable than the classical bonded-particle model for specific applications as the simulation of crack propagation during an indentation test. For a practical standpoint, each cohesive link between a pair of particles  $i$  and  $j$  of radii  $R_i$  et  $R_j$  is defined by a beam element of local Young's modulus  $E_\mu$ , length  $l_\mu \approx r_i + r_j$  and a circular cross-section  $S_\mu$  of radius  $a_\mu$  and planar  $I_\mu$  and polar  $J_\mu = 2I_\mu$  quadratic moments. Typically, for practical reasons, a dimensionless beam radius  $r_\mu > 0$  is introduced:

$$r_\mu = \frac{2a_\mu}{R_i + R_j} \quad (1)$$

Thus,  $S_\mu$  and  $I_\mu$  express as function of  $r_\mu$  as follows :

$$S_\mu = \pi a_\mu^2 = \pi \frac{r_\mu^2}{4} (R_i + R_j)^2 \quad (2)$$

$$I_\mu = \pi \frac{a_\mu^4}{4} = \pi \frac{r_\mu^4}{64} (R_i + R_j)^4 \quad (3)$$

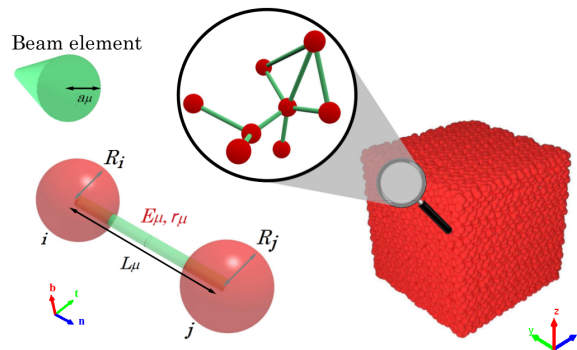


Figure 1: Cohesive beam model

For dense enough particulate systems, the particle size has little effect on the elastic properties of the continuous medium. Thus, the description of the beam model can be reduced to the sole pair of parameters  $E_\mu$  and  $r_\mu$ . Internal cohesive forces are defined by a six-component vector of generalised forces which includes normal and tangential force components and bending and torsion moment ones. This derives from a 6-by-6 matrix system the components of which are function of  $E_\mu$  and  $r_\mu$  parameters and the expression of which is provided in previous contributions [9]. Typically, Newton's second law of motion which includes cohesive and Rayleigh damping forces is solved for each particle over the time using an explicit time integration based on the velocity Verlet scheme.

### 2.3 Macroscopic elastic properties

Macroscopic Young's modulus  $E_M$  and Poisson's ratio  $\nu_M$  of the targeted continuous medium are related to  $E_\mu$  and  $r_\mu$  using the following relations:

$$r_\mu = f(\nu_M) \quad (4)$$

$$E_\mu = g(r_\mu)E_M \quad (5)$$

where  $f$  and  $g$  are polynomial functions the expressions of which are determined using a calibration procedure described in previous works. Note that both functions are function of the main features of the particulate system  $Z$  and  $\phi$  so as the relation between the pairs of parameters  $(E_\mu, r_\mu)$  and  $(E_M, \nu_M)$  is only suitable for given  $Z$  and  $\phi$  values.

### 2.4 Stress field determination

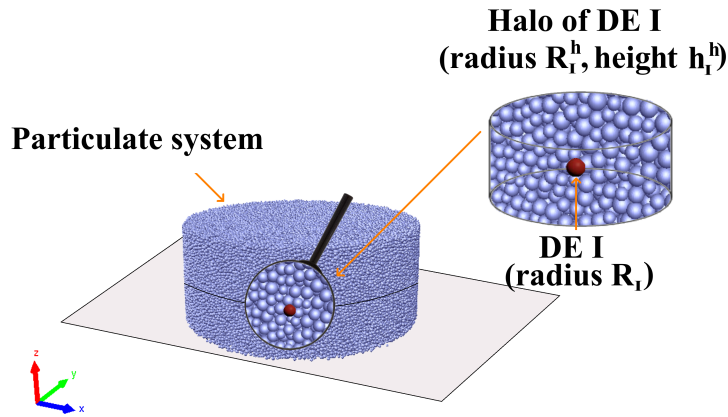


Figure 2: Definition of the halo approach to evaluate stress fields

Stress fields are determined using the halo approach which was proposed by Moukadiri et al. [11] to control variability effects related to the discrete nature of particulate systems. Such a paradigm consists in evaluating stress components related to a given DE I by taking into account the contributions of neighbouring particles in a controlled manner. In the present contribution, the stress formulation in halo approach is based on symmetrised Zhou's formulation of stress tensor:

$$\bar{\sigma}_I^h = \frac{1}{2V_I^h} \sum_{i \in V_I^h} \sum_{j=1}^{Z_i} \frac{1}{2} (\mathbf{f}_{ij} \otimes \mathbf{l}_{ij} + \mathbf{f}_{ji} \otimes \mathbf{l}_{ji}) \quad (6)$$

where  $V_I^h$  is the volume of a geometrical domain surrounding a given particle I.  $Z_i$  is the number of particles in contact with a DE  $i$ ,  $\mathbf{f}_{ij}$  is the interparticle force vector exerted by DE  $j$  on DE  $i$ , and  $\mathbf{l}_{ij}$  is the relative position vector between particles  $i$  and  $j$ . In the present study, a cylindrical halo of radius  $R_I^h$  and height  $h_I^h$  is associated to each particle I of radius  $R_I$  to mimic the cylindrical domain of simulated tablets. Note that, in most cases, if DE I is located far from the domain boundaries,  $V_I^h = \pi R_I^h{}^2 h_I^h$  (else only a part of the cylinder could be considered). Furthermore, as illustrated on Figure 2, each DE center coincides with the centroid of its cylindrical halo.

### 3 Diametral compression test of a cylindrical tablet

#### 3.1 Test configuration

A cylindrical tablet of radius  $R=2\text{cm}$  and height  $h=1.6\text{cm}$  is submitted to a diametral compression as illustrated on Figure 3a. A constant velocity  $v=1\text{mm/min}$  along  $x$  direction is applied to extreme positions where the experimental device is in contact with the sample. Thus, local stress concentrations should be observed close to contact areas but numerical predictions should be also closer to predictions given by Hertz solution at the center of the specimen. Mechanical properties and characteristics of the particulate system come from a previous contribution [12] in which real experiments were led on tablets composed of anhydrous lactose powder (DuraLac<sup>®</sup> H from Meggle). Thus, the density of particles is set to  $1515\text{ kg/m}^3$ , the macroscopic Young's modulus of the sample is  $E_M=5.1\text{GPa}$  and the Poisson's ratio is  $0.24$ . Note that in this previous work, discrete simulations were performed using a particulate system composed of only 10000 DE. In the present work, we handle a granular packing composed of 2 millions spherical particles with an average diameter of  $240\text{ }\mu\text{m}$  which is quite close to the real median particle size  $D_{50}=214\text{ }\mu\text{m}$ . For information purposes, numerical simulations are carried out using a volume fraction of particles  $\phi = 0.64$ , a coordination number  $Z = 7.5$  and microscopic parameters  $E_\mu = 2.469\text{ GPa}$  and  $r_\mu = 0.5$ .

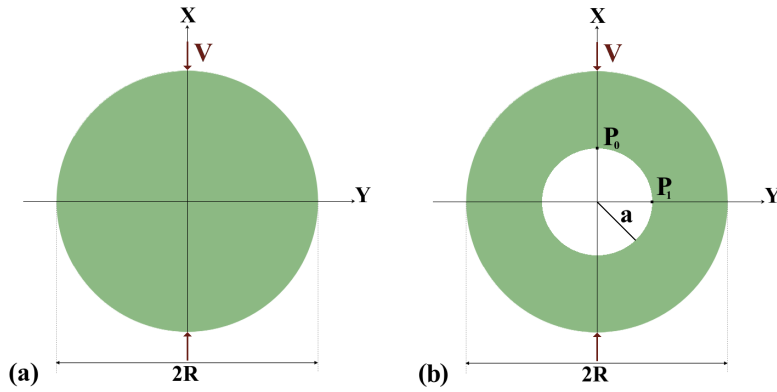


Figure 3: Configuration of the diametral compression test (a) without hole (b) with hole

#### 3.2 Stress fields

$\sigma_{xx}$  and  $\sigma_{yy}$  stresses given by Hertz solution read as follows:

$$\begin{aligned}\sigma_{xx}(x,y) &= -\frac{2F}{\pi h} \left( \frac{(R-x)^3}{\beta_1^4} + \frac{(R+x)^3}{\beta_2^4} - \frac{1}{2R} \right) \\ \sigma_{yy}(x,y) &= -\frac{2F}{\pi h} \left( \frac{y^2(R-x)}{\beta_1^4} + \frac{y^2(R+x)}{\beta_2^4} - \frac{1}{2R} \right)\end{aligned}\quad (7)$$

where  $\beta_1^2 = (R-x)^2 + y^2$  and  $\beta_2^2 = (R+x)^2 + y^2$  and  $F$  is the force applied to the cylindrical tablet. In particular, at the center of coordinates  $(x=0, y=0, z=0)$ ,  $\sigma_{xx}(0,0,0) = -3F/(\pi Rh)$  and  $\sigma_{yy}(0,0,0) = F/(\pi Rh)$  and normalized values  $\sigma_{xx}^* = \sigma_{xx}\pi Rh/F$  and  $\sigma_{yy}^* = \sigma_{yy}\pi Rh/F$  are respectively equal to  $-3$  and  $+1$ . Thus, in absolute values, the stress along the compression direction is three times the one along the tensile direction. Based on previous investigations on the suitable halo size [11, 10], stress values are determined using a halo of radius  $R_1^h=0.08R$  which corresponds to a  $R_1^h/R_1$  ratio of about 13. The height of the halo  $h_1^h$  is set to 0.8 times the height of the cylindrical tablet  $h$  to take into account a maximum number of particles along  $z$  direction without including DE located too close of upper and lower boundary surfaces. Figures 4 and 5 depict the evolution of normalized  $\sigma_{yy}^*$  and  $\sigma_{xx}^*$  stress fields along  $x$  and  $y$  directions respectively in the mid-plane of the cylinder ( $z=0$ ). DEM predictions are compared to theoretical values given by Hertz solution and FEM estimates. Results exhibit a quite good

agreement between the three methods. Thus, at the center of the tablet,  $\sigma_{xx}^*$  and  $\sigma_{yy}^*$  obtained by DEM are respectively -2.808 and 0.973 and quite close to theoretical values -3 and 1, and FEM results -3.071 and 0.928. This highlights the relevance of the choice of halo dimensions for the simulation of stresses fields using DEM in the context of a diametral compression test.

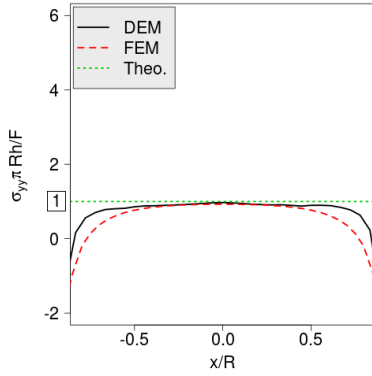


Figure 4: Evolution of normalized  $\sigma_{yy}^*$  stress field along  $x$  direction in the mid-plane of the cylinder

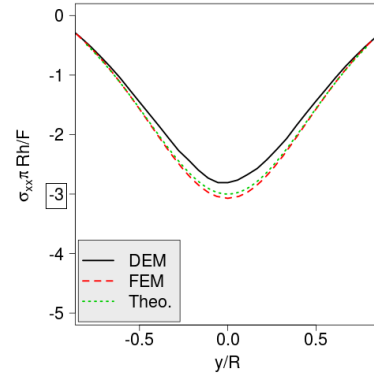


Figure 5: Evolution of normalized  $\sigma_{xx}^*$  stress field along  $y$  direction in the mid-plane of the cylinder

## 4 Diametral compression test of a tablet with a cylindrical hole

### 4.1 Halo definition and determination

We now consider the case of the diametral compression test of a tablet with a cylindrical hole. Figure 3b illustrates the configuration of the test which is based on the same dimensions and properties as discussed in the case of samples without hole. The hole size is controlled by the ratio  $\lambda$  between the radius of the hole  $a$  and the radius  $R$  of the cylindrical tablet. In the present case, the determination of stress fields using the halo definition given in subsection 3.2 is questionable. Indeed, the halo size defined with respect to the radius of the specimen is very large compared to the dimensions of the hole which could be smaller than the halo itself in some cases. As a result, in the present context, we propose to define the halo size with respect to the hole size. Thus, the stress associated to a given DE is determined by considering the contributions of neighbouring particles located in a very restricted area. Nevertheless, such a definition raises another question related to the ratio between halo and DE size which is consequently directly connected to the hole size so as the larger the hole size is the greater the number of particles within the halo is. In other words, in such a concept, the stress field determined using a "large" hole is more representative of a continuous medium than the stress evaluated using a "small" hole. Such a definition is consequently more suitable for particles located close to the hole, especially at  $P_0(a,0,0)$  and  $P_1(0,a,0)$  positions which are associated to  $K_0$  and  $K_1$  SCF and are of prime interest in the present case.  $K_0$  and  $K_1$  SCF are defined as function of the applied force  $F$ , the dimensions  $R$  and  $h$  of the cylindrical tablet and  $\sigma_{xx}$  and  $\sigma_{yy}$  stress values as follows:

$$\begin{aligned} K_0 &= \frac{\sigma_{yy}(a, 0, 0)\pi R h}{F} \\ K_1 &= -\frac{\sigma_{xx}(0, a, 0)\pi R h}{F} \end{aligned} \quad (8)$$

Batista et al. [13] provided a theoretical solution to evaluate  $K_0$  and  $K_1$  as function of the hole size. In particular, the authors demonstrated that  $K_0=6$  and  $K_1=12$  when  $\lambda$  tends to zero. Figure 6 depicts the evolution of  $K_0$  and  $K_1$  SCF as function of the halo size  $R_1^h$  for  $\lambda = 0.4$  and  $h_1^h=0.8h$ . In such a configuration,  $K_0$  and  $K_1$  are theoretically both equal to 13.7. Results exhibit that a too small halo size leads to overestimated values while a too large halo size leads to underestimated SCF. The suitable ratio between the halo radius  $R_1^h$  and the hole radius  $a$  is close to 0.08/0.1. This is quite consistent with the ratio of 0.08 defined between the halo radius  $R_1^h$  and the radius of the cylindrical sample  $R$  in the context of a tablet without hole.

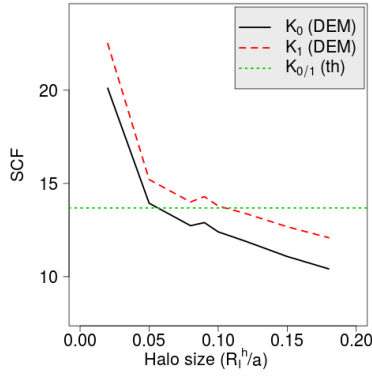


Figure 6: Influence of the halo size on  $K_0$  and  $K_1$  SCF for  $\lambda = 0.4$

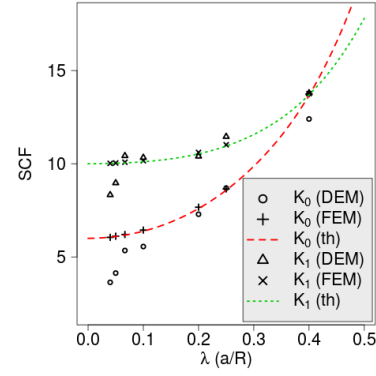


Figure 7: Influence of the hole size on  $K_0$  and  $K_1$  SCF for  $R_1^h=0.1a$

## 4.2 Stress concentration factors

We now aim to evaluate the influence of the dimensionless hole size  $\lambda$  on  $K_0$  and  $K_1$  SCF. Based on previous findings, we consider a halo of radius  $R_1^h=0.1a$  and the height of the cylindrical halo is again set to 0.8 times the height of the cylindrical tablet. Figure 7 shows the evolution curves of  $K_0$  and  $K_1$  SCF as function of  $\lambda$  parameter obtained using DEM, FEM and Batista theoretical approach. First, as verified by previous contributions [14], FEM predictions perfectly fit the theoretical solution whatever the hole size. Thus, as expected,  $K_0$  and  $K_1$  SCF tend to 6 and 12 respectively when  $\lambda$  tends to zero. Second, DEM results exhibit two separate behaviours according to  $\lambda$  parameter. Thus, for a large hole size characterised by a  $\lambda$  parameter higher than 0.1, DEM predictions are quite close to theoretical solutions. By contrast, for a small hole size characterised by a  $\lambda$  parameter lower than 0.1, DEM predictions tend to deviate from theoretical solutions and  $K_0$  and  $K_1$  SCF tend to 3 and 8 respectively. Such results are consistent with some experimental observations [14] which highlighted that a higher force is required to break the cylindrical tablet when  $\lambda \leq 0.1$  and  $\lambda$  tends to zero. This exhibits that  $K_0$  and  $K_1$  SCF are not constant for small holes with  $\lambda \leq 0.1$  contrary to theoretical conclusions. Besides,  $K_0$  value agrees well with the factor 3 taken by Roberts and Rowe [15]. Such findings highlight the ability of the proposed DEM approach to model the transition between a continuous medium and a discrete one with respect to  $\lambda$  parameter. Thus, the case of a cylindrical tablet with a large hole ( $\lambda > 0.1$ ) is more representative of a continuous medium and consequently better modelled by FEM. Conversely, a configuration with a small hole ( $\lambda \leq 0.1$ ) for which the particle size is not negligible compared to the hole size and the hypothesis of a continuous medium is more arguable, is a priori better simulated using a discrete approach. The proposed definition of halo size allows for ensuring the transition between both behaviours in discrete modelling so that a quite suitable result is obtained using DEM independently of  $\lambda$  parameter.

## 5 Conclusions and prospects

In this work, we presented the results of a study on modelling and numerical simulation of mechanical strength of pharmaceutical tablets. Based on DEM, numerical diametral compression test were carried on cylindrical tablets with hole. The influence of the ratio between the hole radius and the tablet one is investigated. The global objective were to study the influence of such default on the mechanical strength of pharmaceutical tablets. The study of influence of the variability at the level the links between the powders on the mechanical resistance will be the subject of a detailed study in the future. A stochastic distribution law of mechanical properties at the scale of contacts will be considered. Before that, the influence of compression parameters process and morphological parameters of powders during settlement step will be studied. This task allows to understand the physical origins of the mechanical strength of tablets.

## References

- [1] E. N. Hiestand, J.E. Wells, C.B. Peot, C.B., J.F. Ochs. *Physical processes of tableting, ?Journal of Pharmaceutical Sciences*, vol. 66, pp. 510-519, Apr. 1977.
- [2] C. Imbert, P. Tchoreloff, B. Leclerc, G. Couarraze. *Indices of tableting performance and application of percolation theory to powder compaction*, Eur. J. Pharm. Biopharm. 44, 273-282, 1997.
- [3] J.M. Whitney, R.J. Nuismer. *Stress fracture criteria for laminated composites contain-ing stress concentrations*, J. Compos. Mater. 8, 253-265, 1974.
- [4] F. Podczek, J.M. Newton. *The implications of the determination of the mechanical strength of powder compacts containing a pre-formed hole*, Powder Technol. 132, 10-15, 2003.
- [5] A.J. Durelli, Y.H. Lin. *Stresses and displacements on the boundaries of circular rings diametrically loaded*, J. Appl. Mech. 53, 213-219, 1986.
- [6] H. Haddad, W. Leclerc, M. Guessasma, C. Pélegris, N. Ferguen, E. Bellenger. *Application of DEM to predict the elastic behavior of particulate composite materials*, Granular Matter, 17, 459-473, 2015.
- [7] D. Moukadiri, W. Leclerc, K. Khellil, Z. Aboura, M. Guessasma, E. Bellenger, F. Druesne. *Halo approach to evaluate the stress distribution in 3D Discrete Element Method simulation: Validation and application to flax/bio based epoxy composite*, Model Simul Mater Sci Eng, 27 (6) (2019).
- [8] W. Leclerc, H. Haddad, M. Guessasma. *On the suitability of a Discrete Element Method to simulate cracks initiation and propagation in heterogeneous media*. Int J Solids Struct, 108 (2017), pp. 98-104.
- [9] W. Leclerc. *Discrete Element Method to simulate the elastic behavior of 3D heterogeneous continuous media*, International Journal of Solids and Structures, 86-102(121), 2017.
- [10] W. Leclerc, A. Ammar, D. Moukadiri, T. Dridi, M. Guessasma. *Halo approach to model cracks initiation and propagation in 3D Discrete Element Method simulation of homogeneous and heterogeneous materials*, Composite Structures, 113222(259), 2021.
- [11] D. Moukadiri, W. Leclerc, K. Khellil, Z. Aboura, M. Guessasma, E. Bellenger, F. Druesne. *Halo approach to evaluate the stress distribution in 3D discrete element method simulation : Validation and application to flax/bio based epoxy composite*, Modelling and Simulation in Materials Science and Engineering, 065005(27), 2019.
- [12] Z. Afrassiabian, W. Leclerc, M. Guessasma, K. Saleh. *Numerical simulation of mechanical resistance of wet and dry powder cakes*, Powder Technology, 45-54(371), 2020.
- [13] M. Batista, J. Usenik. *Stresses in a circular ring under two forces acting along a diameter*, Journal of Strain Analysis, 75-78(31), 1996.
- [14] B. Croquelois, J. Girardot, J.B. Kopp, C. Cazautets, P. Tchoreloff, V. Mazel. *Breaking pharmaceutical tablets with a hole: Reevaluation of the stress concentration factor and influence of the hole size*, Powder Technology, 126-132(317), 2017.
- [15] R.J. Roberts, R.C. Rowe. *Brittle fracture propensity measurements on "tablet-sized" cylindrical compacts*, Journal of Pharmacy and Pharmacology, 526-528(38), 1986.